Alleviation of chronic pain following rat spinal cord compression injury with multimodal actions of huperzine A

Dou Yu[a,b,1], Devang K. Thakor[a,b,1], Inbo Han[a,b], Alexander E. Ropper[a,b], Hariprakash Haragopal[a,b], Richard L. Sidman[c,2], Ross Zafonte[d], Steven C. Schachter[c,e], and Yang D. Teng[a,b,d,2]

[a]Department of Neurosurgery, Harvard Medical School/Brigham and Women's Hospital/Boston Children's Hospital, Boston, MA 02115; [b]Division of SCI Research, Veteran Affairs Boston Healthcare System, Boston, MA 02130; [c]Department of Neurology, Harvard Medical School/Beth Israel Deaconess Medical Center, Boston, MA 02215; [d]Department of Physical Medicine and Rehabilitation, Harvard Medical School/Spaulding Rehabilitation Hospital, Boston, MA 02114; and [e]Center for Integration of Medicine and Innovative Technology, Boston, MA 02114

Contributed by Richard L. Sidman, January 2, 2013 (sent for review October 11, 2012)

Diverse mechanisms including activation of NMDA receptors, microglial activation, reactive astrogliosis, loss of descending inhibition, and spasticity are responsible for ~40% of cases of intractable neuropathic pain after spinal cord injury (SCI). Because conventional treatments blocking individual mechanisms elicit only short-term effectiveness, a multimodal approach with simultaneous actions against major pain-related pathways may have value for clinical management of chronic pain. We hypothesize that [-]-huperzine A (HUP-A), an alkaloid isolated from the club moss *Huperzia serrata*, that is a potent reversible inhibitor of acetylcholinesterase and NMDA receptors, could mitigate pain without invoking drug tolerance or dependence by stimulating cholinergic interneurons to impede pain signaling, inhibiting inflammation via microglial cholinergic activation, and blocking NMDA-mediated central hypersensitization. We tested our hypothesis by administering HUP-A i.p. or intrathecally to female Sprague–Dawley rats (200–235 g body weight) after moderate static compression (35 g for 5 min) of T10 spinal cord. Compared with controls, HUP-A treatment demonstrates significant analgesic effects in both regimens. SCI rats manifested no drug tolerance following repeated bolus i.p. or chronic intrathecal HUP-A dosing. The pain-ameliorating effect of HUP-A is cholinergic dependent. Relative to vehicle treatment, HUP-A administration also reduced neural inflammation, retained higher numbers of calcium-impermeable GluR2-containing AMPA receptors, and prevented Homer1a up-regulation in dorsal horn sensory neurons. Therefore, HUP-A may provide safe and effective management for chronic postneurotrauma pain by reestablishing homeostasis of sensory circuits.

botanical medicine | hyperalgesia

Neuropathic pain is one of the most debilitating sequelae of neurotrauma and is an unmet clinical need for at least 40% of patients with spinal cord injury (SCI) (1). Administration of conventional drugs has shown only various degrees of short-term efficacy in reducing at- and/or below-injury-level hypersensitivity after SCI by acting on individual pathways to inhibit descending facilitation of pain-transmission neurons (2), activate inhibitory interneurons in the spinal cord (2, 3), mitigate firing of pain-transmission neurons (3–7), or impede inflammation triggered by the activation of astrocytes and microglial cells (8). The diversity of mechanisms and potential targets for intervention may be partially responsible for the difficulty in developing therapeutics that can provide long-term efficacy. Therefore we postulated that devising a multimodal treatment with potent, defined simultaneous effects on multiple pain-related pathways might be an effective concept for clinical management of neuropathic pain.

Given the potential roles of cholinergic agonists (9, 10) and antagonists of NMDA-subtype glutamate receptors (10, 11) in the treatment of neuropathic pain, we hypothesized that [-]-huperzine A (HUP-A) (Fig. 1*A*), a naturally occurring *Lycopodium* alkaloid isolated from the Chinese club moss, *Huperzia serrata* (Fig. 1*B*) that has potent reversible inhibitory action on acetylcholinesterase (AChE) (Fig. 1*C*) (10, 12) and NMDA receptors (Fig. 1*D*) (13), might be an exceptional prospect for multimodal treatment of SCI-induced neuropathic pain. We tested whether HUP-A–derived NMDA blockade and the overall HUP-A–derived augmentation of cholinergic neurotransmission arising from AChE inhibition might be harnessed specifically to stage a multifocal intervention in post-SCI pain pathways because (*i*) antagonism of NMDA receptor prevents the post-SCI hyperexcitability of neurons in the dorsal horn (DH) of the spinal cord that feature a wide, dynamic range of pain transmission (7); (*ii*) activation of presynaptic α3β2 nicotinic ACh receptors (nAChR) minimizes release of glutamate from C-fiber terminals in the DH that are involved in nociceptive neurotransmission (14); (*iii*) activation of GABAergic interneurons via stimulation of their M2 and M4 muscarinic ACh receptors (mAChR), in turn, inhibits presynaptic release of glutamate from primary afferent axons (15, 16); (*iv*) activation of the α4β2 nAChR on GABAergic inhibitory interneurons mitigates the firing of secondary spinothalamic pain transmission neurons (17); and (*v*) stimulation of the α7 nAChR on microglial cells blocks their activation, ameliorating neuroinflammation (18, 19). The primary goal of our study is to develop a class of therapeutics for the management of chronic neuropathic

Significance

Neuropathic pain, one of the most debilitating sequelae of neurotrauma, is an unmet clinical need for at least 40% of patients with spinal cord injury (SCI). We demonstrate that [-]-huperzine A (HUP-A), a naturally occurring *Lycopodium* alkaloid isolated from the Chinese club moss, *Huperzia serrata*, with potent reversible inhibitory action on acetylcholinesterase and *N*-methyl-D-aspartate glutamate receptors, offers an exceptional prospect for multimodal treatment of SCI-induced neuropathic pain in rats. HUP-A restores homeostasis of central sensory neurocircuitry without invoking drug tolerance and dependence or respiratory suppression. We therefore conclude that multimodal actions provide a fresh translational approach to reduce chronic pain.

Author contributions: D.K.T., R.Z., S.C.S., and Y.D.T. designed research; D.Y., D.K.T., I.H., A.E.R., H.H., and Y.D.T. performed research; D.Y., D.K.T., R.L.S., R.Z., S.C.S., and Y.D.T. analyzed data; and R.L.S., R.Z., S.C.S., and Y.D.T. wrote the paper.

Conflict of interest statement: S.C.S. is an inventor on a patent for the use of huperzine for treatment of neuropathic pain, which is licensed by Harvard Medical School to Insero Health, Inc., in which S.C.S. holds less than 5% equity and for which he serves as chair of the scientific advisory board.

Freely available online through the PNAS open access option.

[1]D.Y. and D.K.T. contributed equally to this work.

[2]To whom correspondence may be addressed. E-mail: richard_sidman@hms.harvard.edu or yang_teng@hms.harvard.edu.

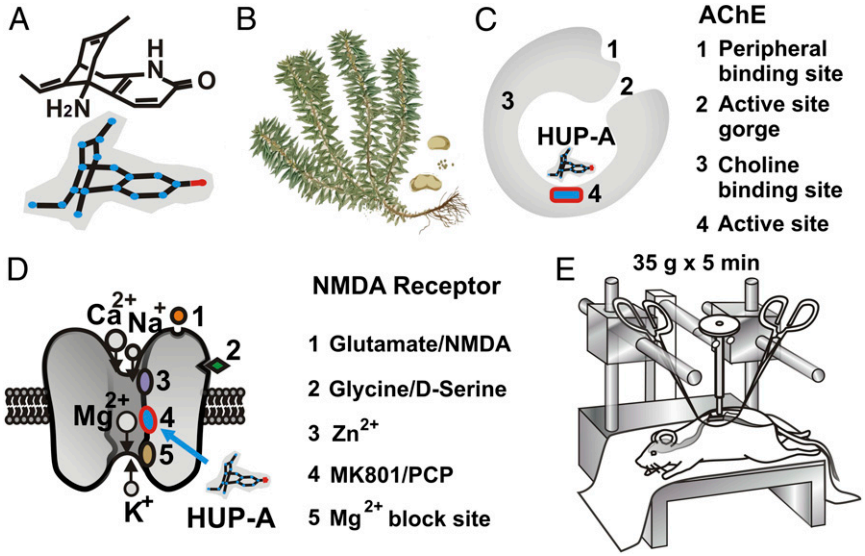

Fig. 1. HUP-A is a natural alkaloid extract. HUP-A's molecular structure is presented in (*A*) from the club moss *Huperzia serrata* (*B*) that is a potent, highly specific, and reversible inhibitor of AChE (*C*) as well as a noncompetitive partial antagonist of the NMDA receptor (*D*). A reproducible moderate static-compression SCI model maintaining 35 g of static weight on the dorsal surface of T10 spinal cord for 5 min was used for the present study (*E*).

pain that aims to restore homeostasis of the sensory neurocircuitry by simultaneous multimodal mechanisms without invoking drug tolerance and dependence or respiratory suppression. HUP-A has been used for centuries in herbal medicine to treat inflammatory and other diseases (10, 12), has demonstrated effectiveness in inhibiting hypersensitivity triggered by peripheral neuropathy (20), and has been studied in phase II clinical trials for Alzheimer's disease in the United States (11). We tested whether HUP-A regimens might translate into an effective and safe therapy for neuropathic pain following SCI in adult female rats (21–23).

Results

Post-SCI Hypersensitivity to Mechanical Stimuli. To assess the potential therapeutic effect of HUP-A, we first used our clinically relevant model of moderate, static-compression SCI (Fig. 1*E*) to profile reproducible post-SCI mechanical hypersensitivity in both the fore- and hindpaws of experimental rats. In a modified von Frey filament assay (Fig. 2*A*), the pre-SCI paw-withdrawal sensitivity threshold was 0.63 ± 0.06 g for the forepaws and 2.00 ± 0.33 g for the hindpaws ($n = 4$; Fig. 2*B*). In the acute phase after SCI (i.e., 24 h after lesion, without treatment), the force required to trigger a withdrawal response increased drastically, to >3 g for the forepaws and >50 g for the hindpaws (day 1 after SCI, Fig. 2*B*). The lack of response in the acute phase is attributable to "spinal shock" associated with the transient shutdown of sensorimotor function in the spinal cord acutely after SCI (24). In the subacute and chronic phases after injury, the withdrawal threshold decreased gradually to below the pre-SCI level in the forepaws (0.11 ± 0.02 g in week 2, $P < 0.01$, and 0.15 ± 0.01 g in week 3, $P < 0.03$; $n = 4$). The hindpaws took a week longer to develop hypersensitivity (1.97 ± 1.17 g in week 2, $P > 0.05$, and 0.47 ± 0.10 g in week 3, $P < 0.05$; $n = 4$); the results in both paws indicate the development of persistent hypersensitivity to mechanical stimuli (Fig. 2*B*).

To evaluate pharmacological specificity and potential side effects of systemic HUP-A administration, following a sequential design with adequate drug washout intervals (i.e., >5× $t_{1/2}$), we injected three doses of HUP-A i.p. following preinjection of an equivolume of saline in the same rats as self-control in week 4 after SCI (10). HUP-A (500, 167, 50 μg/kg, i.p.; $n = 4$ rats per group) induced dose-dependent anti-hypersensitivity (Fig. 2 *C* and *D*). Additionally, after drug administration fine muscle tremors, primarily in the forepaw digits, were observed, indicating systemic HUP-A–mediated AChE inhibition at the neuromuscular junction (10, 12); however, we did not observe any worsening of the hindlimb muscle spasticity that typically develops 3–4 wk after lower thoracic SCI (24). This sign persisted for ∼0.2–2 h in the group with the highest dose of HUP-A. In contrast, the analgesic effects of HUP-A lasted much longer, averaging up to 6 h with bolus i.p. delivery of HUP-A (500 μg/kg; Fig. 2 *C* and *D*). We observed no other isolated or cumulative adverse effects and particularly no effects representing gastrointestinal hyperactivity (23).

Continuous Intrathecal Administration of HUP-A Induces Sustainable Suppression of Post-SCI Hypersensitivity. We next tested a continuous drug-delivery regimen with a s.c.-implanted osmotic pump that delivered HUP-A directly and continuously into the intrathecal (i.t.) space at L5–L6 for 2 wk (0.5 μL/h × 24 h × 14 d; total dose: 90 μg/168 μL) (Fig. 3*A*), with the aim of maintaining the long-term effect of central anti-hypersensitivity and preventing systemic side effects (20). Continuous i.t. delivery of HUP-A via the osmotic pump effectively eliminated the forepaw and hindpaw hypersensitivity to mechanical stimuli. A strong analgesic effect was noted between weeks 1 and 3 after pump implantation: The post–HUP-A treatment sensitivity threshold was significantly higher (Fig. 3 *E–H*) ($n = 7$ per group) than the pretreatment/post-SCI baseline sensitivity thresholds of 0.60 ± 0.04 g and 2.00 ± 0.18 g for the fore- and hindpaws, respectively (Fig. 3 *C* and *D*). The anti-hypersensitivity and analgesic effects were HUP-A dependent, because the effect was first spotted ∼24 h after pump implantation (Fig. 3 *E–H*), reflecting the time needed for HUP-A to course through the microtubing before entering the i.t. space (additional details are given in *Materials and Methods*), and a return of hypersensitivity was observed 2 wk after depletion of HUP-A from the osmotic pump (i.e., 4 wk after s.c. pump insertion). However, readministration of the same dose reestablished the anti-hypersensitivity effect of HUP-A without apparent tolerance or adverse effects (Fig. 3 *E* and *F*; note: the effectiveness of the second HUP-A pumping also lasted for ∼3 wk). To check whether HUP-A's augmentation of central muscarinic activation of cholinergic transmission indeed played a definitive role in managing hypersensitivity, we administered

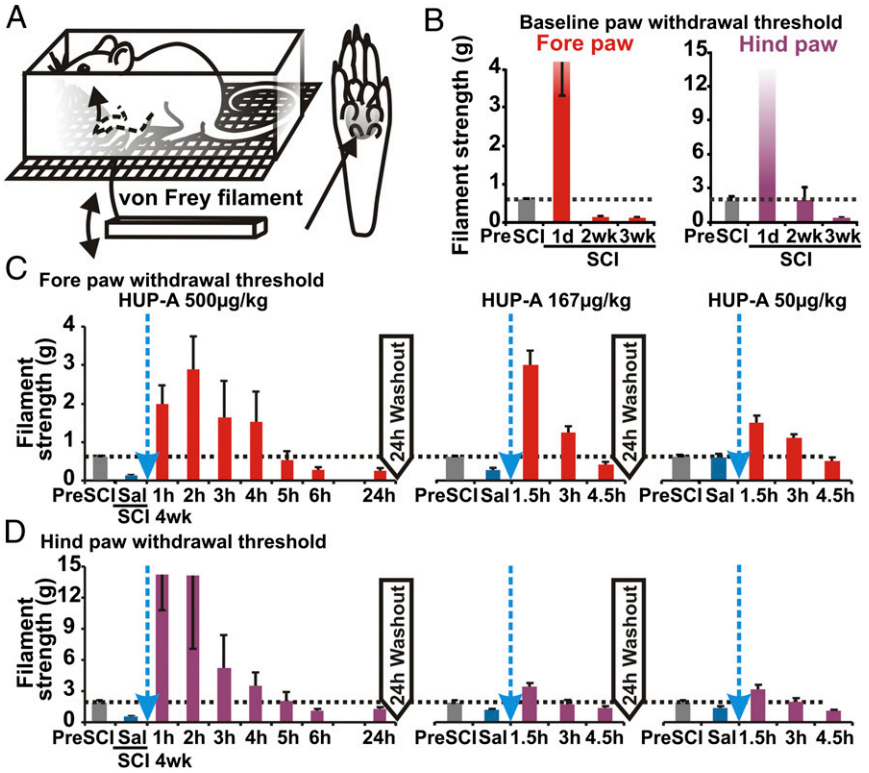

Fig. 2. (*A*) The post-SCI chronic development of above-injury-level and below-injury-level hypersensitivity was evaluated with a modified von Frey filament test, as diagrammed. The forepaw- and hindpaw-withdrawal thresholds to von Frey filaments of several stiffnesses were tested in acclimated and resting conscious rats. The paw area probed by the filament is shaded in gray and indicated by the long arrow. (*B*) Baseline data of changes in the paw-withdrawal threshold over the study's time course. (*C* and *D*) The effect is dose dependent. I.p. injection of varying doses of HUP-A resulted in reproducible anti-hypersensitivity effects, i.e., increased withdrawal thresholds of the forepaws (*C*) and hindpaws (*D*), in the chronic stage of SCI (i.e., 4 wk after injury). Sal, saline.

i.t. bolus doses (15 μg/10 μL) of atropine, a nonselective muscarinic cholinergic antagonist (Fig. 3*B*), into SCI rats 20 d after onset of HUP-A infusion (i.e., 5 d after the exhaustion of the contents of the HUP-A pump). The timing of this test allowed a cleaner assessment of HUP-A's anti-hypersensitivity capability derived from cholinergic activation per se, because the anti-central pain effect of HUP-A mediated by NMDA antagonism diminishes swiftly after the end of drug administration (i.e., when HUP-A infusion became exhausted 2 wk after pump insertion) (20, 21). Injection of atropine indeed abolished HUP-A–mediated anti-hypersensitivity immediately, indicating that the continued analgesic effect observed in week 3 after minipump implantation resulted largely from cholinergic agonism via HUP-A's longer-lasting inhibition of AChE (Fig. 3 *E*–*H*, *Right*) (20). Interestingly, although the observed increase in paw-withdrawal thresholds in response to mechanical stimuli is consistent with the observed effects on nonnoxious paw pressure and nociceptive pinch reflexes during the second week of HUP-A infusion (Fig. 3 *D*, *G*, and *H*), open-field locomotor performance [measured by the Basso–Beattie–Bresnahan (BBB) score; Fig. 3*I*] and coordinated body posture control (measured by the inclined plane angle threshold for maintaining head-downward posture; Fig. 3*J*) were not affected significantly by i.t. administration of HUP-A.

Histopathology and Immunocytochemical Analyses of the Spinal Cords. Although gross pathology at the lesion epicenter assessed by solvent blue and hematoxylin staining (Fig. 4*A*) did not demonstrate significant differences in spared tissue volume (Fig. 4*B*) or in the number of surviving motor neurons (Fig. 4*C*), further immunocytochemical (ICC) analyses revealed that specific neuroinflammation markers were differentially expressed in the i.t. HUP-A–treated spinal cords and saline-treated controls, especially in the cervical and lumbar regions that receive sensory inputs from the fore- and hindpaws, respectively (25–27). Expression of GFAP, a classic marker of astrocytes whose expression is increased markedly in reactive gliosis and neuroinflammation (26, 27), was observed in all chronically injured spinal cords. However, rats treated with i.t. HUP-A demonstrated significantly reduced GFAP immunoreactivity in cervical and lumbar spinal cord regions (Fig. 5*A*), as well as a significantly lower immunoreactivity level for CD68, a marker for activated microglia and macrophages, in the lumbar spinal cord (26, 27); no effect of HUP-A on cervical CD68 immunoreactivity was detected (Fig. 5*B*). Immunoreactivity for the inducible form of nitric oxide synthase (iNOS), a critical neuroinflammatory mediator expressed by immune cells and microglia (27), was significantly lower in the cervical (Fig. 5*C*, red immunoreactivity) and lumbar (Fig. 5*D*) spinal cords of the HUP-A–treated group than in the saline-treated controls. Immunoreactivity for CD86, which is expressed by M1 macrophages that have a detrimental role after SCI (28), was reduced significantly in cervical (Fig. 5*E*, green cells) and lumbar (Fig. 5*F*) regions of the HUP-A–treated group compared with controls, whereas immunoreactivity for arginase1, which is expressed by M2 macrophages that have a beneficial role after SCI (28), was comparable in the cervical and lumbar spinal cord in both groups (Fig. 5 *E* and *F*, red cells). The differences in the immunoreactivity profiles of cervical CD68, iNOS, and CD86 may carry further mechanistic information and should be investigated systematically in future studies (29).

The immunoreactivity of the oligodendrocyte markers CNPase (Fig. 5 *G* and *H*) and myelin basic protein (MBP) (Fig. 5 *I* and *J*) demonstrated significantly increased preservation of myelin in the lumbar white matter of HUP-A–treated rats, suggesting that i.t. HUP-A treatment did not trigger myelin toxicity, as has been reported for some prototype NMDA antagonists (30). Instead,

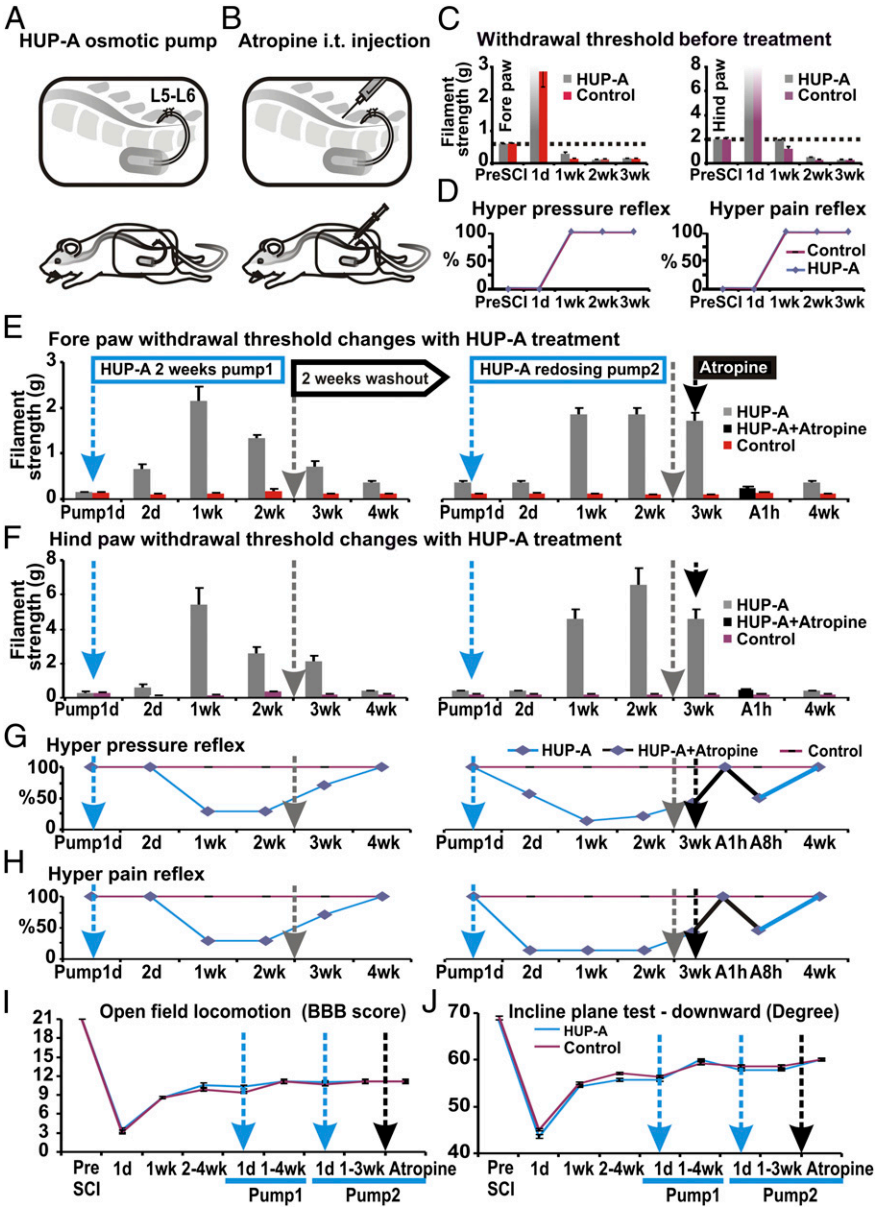

Fig. 3. By using an osmotic pump-mediated i.t. delivery, we provided more targeted administration of HUP-A. (*A*) Schematic representation of the s.c.-implanted osmotic pump for i.t. delivery. (*B*) Schematic representation of i.t. injection of atropine. (*C*) Baseline data before and after SCI: changes in paw-withdrawal threshold in response to a modified von Frey filament test. (*D*) Baseline data before and after SCI: changes in paw-withdrawal threshold in response to conventional pressure and painful spinal reflex tests. (*E–H)* In *E* and *F*, the forepaws and hindpaws demonstrated durable (i.e., up to 3 wk after HUP minipump implantation) increases in the sensory threshold to mechanical stimuli. (*E–H, Far Right*) An i.t. bolus injection of atropine (*B*) swiftly and temporarily blocked the anti-hypersensitivity effect of HUP-A. In *G* and *H*, hind-limb sensory reflexes support the findings obtained for the paw-withdrawal threshold. However, *I* and *J* indicate that HUP treatment did not improve locomotion as evaluated with the open-field locomotion test (BBB score) and the head-downward inclined plane test (24).

HUP-A protected against demyelination in chronic SCI. However, immunoreactivity levels of CNPase, a marker of immature oligodendrocytes, were comparable in the cervical spinal cords of the HUP-A– and saline-treated groups (Fig. 5*H*), possibly because immature oligodendrocytes are less involved in chronic demyelination after SCI. Moreover, we did not find a significant difference in immunoreactivity levels of neurofilament M or H in epicenter tissue sections from HUP-A–treated and control rats (Fig. 5 *K* and *L*). These findings collectively support the hypothesis that chronic administration of HUP-A does not introduce further toxicity in the injured spinal cord and that HUP-A treatment, although not triggering axonal regeneration (Fig. 5 *K* and *L*), protects myelin against the chronic damage resulting from neuroinflammation that is mediated largely by locally activated microglia and astroglia and by macrophage invasion (25–29).

To explore further the mechanistic basis for the observed benefits of the HUP-A treatment, we evaluated the immunoreactivity levels for the GluR2 (also called "GluR-B") subunit of the AMPA receptor, which is Ca^{2+} impermeable and is in balance with numbers of Ca^{2+}-permeable GluR1 subunits to regulate Ca^{2+} permeability in DH neurons where nociceptive relaying/processing occurs (31). Average GluR2 immunoreactivity was significantly higher in the cervical and lumbar spinal cords of the HUP-A–treated group (Fig. 6 *A* and *B*), suggesting that HUP-A–activated cholinergic interneurons might have helped reduce the post-SCI loss of GluR2-expressing neurons that is partially responsible for the development of hypersensitivity (*Discussion* and refs. 31 and 32). More support for this notion is derived from our immunoreactivity data on the nociceptive mediators neurokinin-1 receptor (NK1R) (green immunoreactivity, Fig. 6 *C* and *D*) and calcitonin receptor-like receptor (CRLR) (red immunoreactivity, Fig. 6 *C* and *D*). Both markers were decreased significantly in the cervical and lumbar DH spinal cord of the HUP-A–treated rats. Additionally, immunoreactivity for substance P, a nociceptive neurotransmitter, was decreased significantly in cervical and lumbar spinal cord DH regions of the HUP-A–treated rats. Immunoreactivity for the immediate early gene (IEG) cFos, which is increased in neurons with enhanced activity and is used frequently as a marker of neuronal activation in neuropathic pain, was decreased sig-

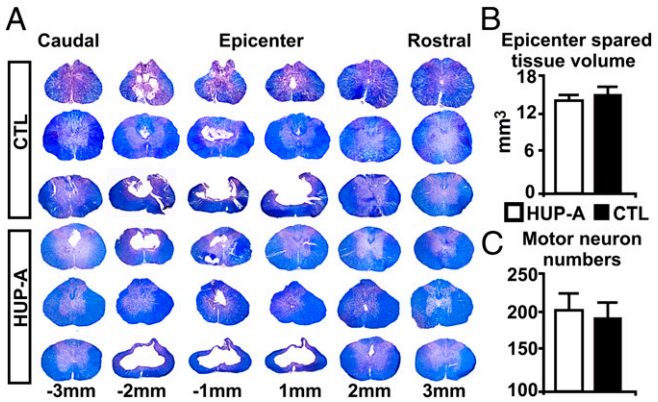

Fig. 4. Lesion epicenter histopathology (S/H staining) (*A*) was similar in the HUP-A–treated and saline-treated control (CTL) spinal cords based on analysis of the spared tissue volume in the epicenter (*B*) and the number of surviving motoneurons in the region surrounding the epicenter. Motor neuron numbers (mean ± S.E.) were calculated by summing motor neuron numbers of 6 coronal sections (20 μm) selected from each mm of tissue rostral and caudral to the epicenter (i.e., -3 – 3 mm) and then averaged (n = 7/group) (*C*). CTL, control. (Magnification: 5×).

nificantly in laminae I–III of the cervical and lumbar DH spinal cord in the HUP-A–treated group (Fig. 6 *G* and *H*). Similarly, Homer1a, an activity-dependent inducible dominant-negative form of the linking protein that can disrupt the mGluR-signaling complex and regulate nociceptive plasticity at spinal synapses (33), was significantly lower in the cervical and lumbar DH of HUP-A–treated rats than in controls (Fig. 6 *I* and *J*). This result suggests that, with HUP-A treatment, DH sensory neurons became less activated by nociceptive signaling. Additionally, group average immunoreactivity intensity of the neurotrophin receptor p75NTR also was significantly weaker in the cervical and lumbar DH of the HUP-A–treated rats (Fig. 6 *K* and *L*) than in the control group, indicating decreased local sensory neurite sprouting. This decrease also may contribute to the observed anti-hyperalgesic effect of HUP-A, because aberrant neurite sprouting in the spinal cord contributes to the onset and maintenance of neuropathic pain in other clinical settings such as postherpetic or postcrush neuralgia (34).

Discussion

Pain is one of the most common and debilitating sequelae of spinal cord trauma, as illuminated by a longitudinal cohort study in which 81% of patients reported pain within the first 5 y after SCI, and 58% reported their pain as severe or excruciating (1). Despite its high prevalence and severe impact on patient quality of life, management of SCI pain (and neuropathic pain in general) remains an unmet clinical challenge because available therapies are neither satisfactorily effective nor free of side effects (35). The problem may lie partially in the diversity of underlying pathophysiological mechanisms, because most therapeutic approaches focus on a single target that often serves a single function, predominantly neurotransmission. Thus, today's therapies typically address only part of the pathological process and fail to prevent some affected targets from direct compensation or replacement by alternate pathways; commonly, the patient gradually becomes insensitive/tolerant to the treatment (35). Development of drug dependence is an additional problem. Furthermore, neuropathic pain is difficult to model and measure in experimental settings, and therapeutic approaches that are effective in laboratory models often do not translate directly to patients (25, 35).

In the present study, we demonstrate that our recently developed thoracic static compression SCI model induces chronic mechanical hypersensitivity/hyperalgesia suggestively similar to clinical neuropathic pain. Animal models of neuropathic pain after SCI are rare, so that a standard battery of evaluable neuropathic pain behaviors specific to rodent SCI does not truly exist (29, 36). As an index of neuropathic pain below the SCI level, we used hindpaw hypersensitivity, which is widely accepted as a general measure of rodent neuropathic pain behavior in peripheral mononeuropathy models involving injury to hindlimb nerves but also has been used in SCI models (2, 4–6, 29). The moderate degree of compression injury in our model appeared to be ideally suited to the measurement of hindpaw-withdrawal thresholds, because the return of reflexive hindpaw function before reaching the chronic injury phase (Fig. 3 *G* and *H*) made the chosen sensory behavioral tests feasible. We also expanded the behavioral analysis by including spinal reflexes indicative of somatosensory changes, spasticity, and forepaw-withdrawal thresholds to address hypersensitivity at, above, and below injury level that is unique to SCI pain (24). Despite the high clinical relevance (as described above, at-injury-level pain is more prevalent than below-injury-level pain after SCI), these outcome measures have not, to our knowledge, been applied comprehensively to characterize animal models of traumatic SCI, although several studies have probed the dorsal dermatome over the lesion site to screen for at-level hypersensitivity (3, 6). The clinical relevance of our selected outcome measures is underscored further by our injury model itself, which is designed specifically to mimic the mechanics of the most prevalent type of pain-causing SCI in humans by applying a sustained, moderate static compression to the dorsal surface of the spinal cord of adult female rats, which are used routinely in standardized SCI models and are known to develop mechanical hypersensitivity more rapidly and to a higher extent than male rats (24, 26, 37). We consider that this SCI model and the outcome measures introduced in this report provide a particularly appropriate opportunity to identify therapeutic targets for SCI neuropathic pain that may be translatable to the clinic (36).

On investigating potential therapeutics in this context, we found that rodent indices of neuropathic pain above and below the SCI level indeed were reversed via apparently multimodal effects with either bolus systemic or sustained central administration of HUP-A (Figs. 3–6). The anti-hypersensitivity effect of systemic HUP-A treatment is dose dependent, and the definitive beneficial impact of chronic i.t. infusion of HUP-A in our model disappeared ~7 d after the steadily administered HUP-A ended, but the effect was re-established completely and was sustained when the drug pump was restocked. The contrasts between data on the HUP-A and control treatments suggest that the sensory behavioral effect observed in post-SCI rats is attributable directly to the HUP-A treatment. Moreover, HUP-A did not induce drug tolerance or respiratory suppression, major drawbacks of narcotic analgesics (38). Although the highest systemic dose of HUP-A triggered transient peripheral cholinergic overactivation (i.e., fine muscle tremor in the forepaw digits) in addition to a strong anti-hypersensitivity effect, it did not worsen hindlimb spasticity, and neither systemic nor central/local HUP-A treatment in our experiments caused any of the other side effects reported for high doses of HUP-A in neuroprotection studies (11, 21) or associated with prototype NMDA antagonists (30). Therefore, HUP-A, alone or in combination with its synthetic stereoisomer [+]-huperzine-A (11, 21), appears to merit attention in efforts to develop a safe and effective therapy for neuropathic pain of SCI and perhaps for traumatic brain injury and other neurological disorders.

Previously, i.t. HUP-A was shown by members of our group and collaborators to decrease hindpaw hypersensitivity in a rat model of persistent pain after formalin injection into the hindpaws, and this effect was reversed partially by i.t. administration of atropine, a muscarinic antagonist (20). We now have con-

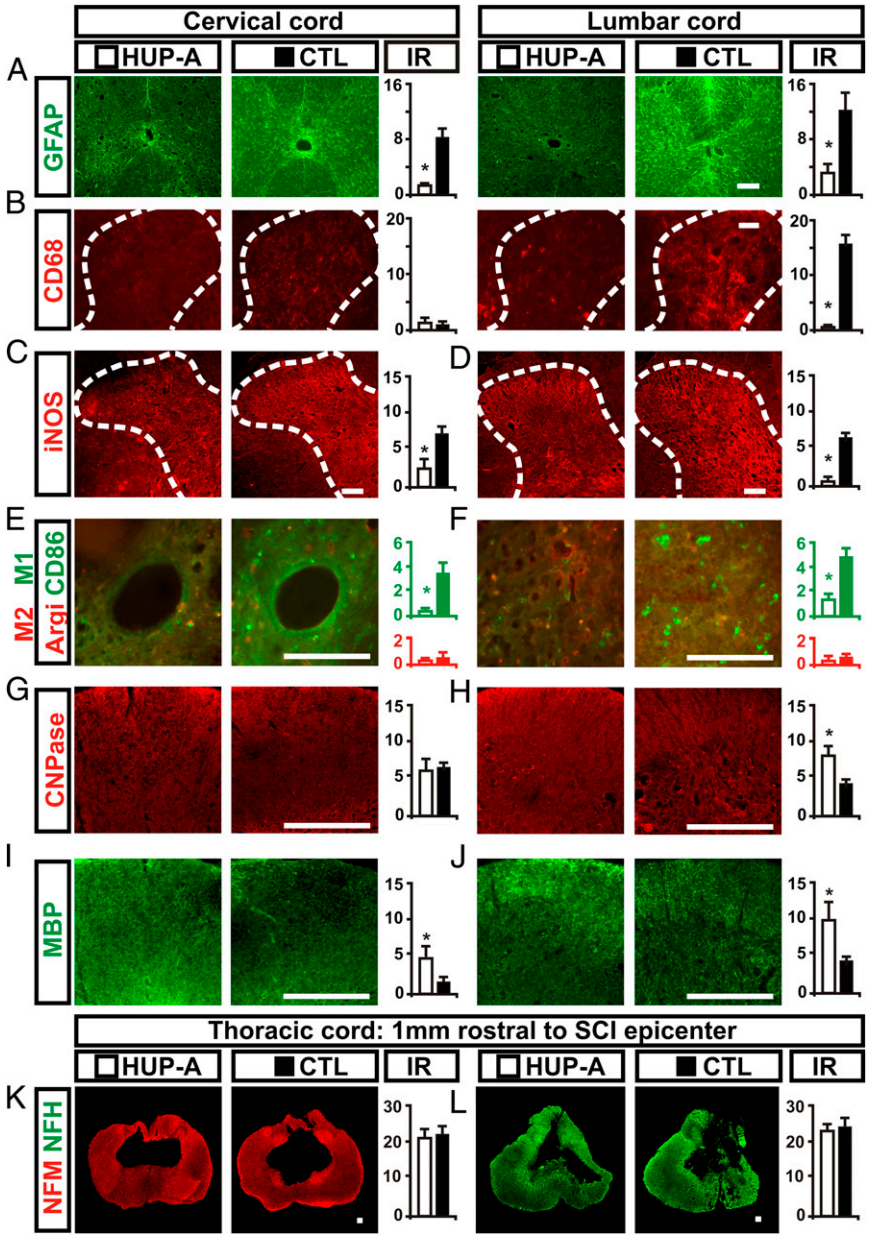

Fig. 5. Neuroinflammation and reactive astrogliosis developed in the cervical and lumbar spinal cord (i.e., regions rostral and caudal to the lesion site, respectively) as evidenced by strong expression of GFAP (*A*); activation of microglia (CD68 is a marker for activated microglia and macrophages) (*B*); expression of iNOS (*C* and *D*); and invasion of M1 macrophages (*E* and *F*) as determined by CD86 staining. HUP-A administration significantly ameliorated all indices of neuroinflammation. However, no changes were observed for immunoreactivity scales of the beneficial M2 macrophages (Arginase, Argi stain). (*G–J*) HUP-A administration protected white matter (WM) tissue, i.e., mitigating the chronic loss of WM myelin (assessed by immunocytochemistry against oligodendrocytic markers, MBP and CNPase), evident in the control group. Chronic HUP-A administration significantly preserved the myelin in the WM compared with the CTL group. (*K* and *L*) Comparison of expression levels immunoreactivity (IR) of neurofilaments M (NFM: (*K*) and H (NFH) (*L*) in transverse epicenter sections from the HUP-A–treated and control (CTL) groups (i.t.; $n = 7$ per group). Because there is no statistical difference between the two groups in the average total pixel numbers per section (768,908 ± 96,330 vs. 752,678 ± 67,401 pixels; $n = 3$ sections per rat; $n = 7$ rats per group; $P > 0.05$, Student t test), the percentages of NFM^+ (*K*, red) or NFH^+ (*L*, green) pixels within the total image field of the white matter were measured and compared. The result suggests that there is no significant difference in neurite presence or regeneration in the spared tissue around injury epicenters. $^*P < 0.05$, Student t test. (Scale bars: 100 μm.)

firmed that i.t. atropine administration per se also could partially block the effect of HUP-A on post-SCI hypersensitivity (Fig. 3). However, we tested the effect of atropine only toward the end of the third week of continuous HUP-A i.t. infusion; in future studies atropine's impact also should be measured earlier, at the peak effect time of HUP-A treatment. Our result suggests that HUP-A has a cholinergic inhibitory action on DH pain transmission, possibly through the activation of M2 and M4 mAChRs on GABAergic inhibitory interneurons that mitigate the release of primary afferent-derived glutamate in the DH (15, 16). The decrease in nociceptive neurotransmission likely was mediated also by the observed immunoreactivity decrease in substance P from primary afferents onto second-order DH neurons (Fig. 6 *E* and *F*). Cholinergic signaling through mAChRs has been reported to decrease the release of substance P in the rat dorsal spinal cord in response to acute noxious stimulation of the tail (39) and to inhibit pain-transmitting spinothalamic and thalamic neurons (17, 40). Although cholinergic agonists for pain control are poorly

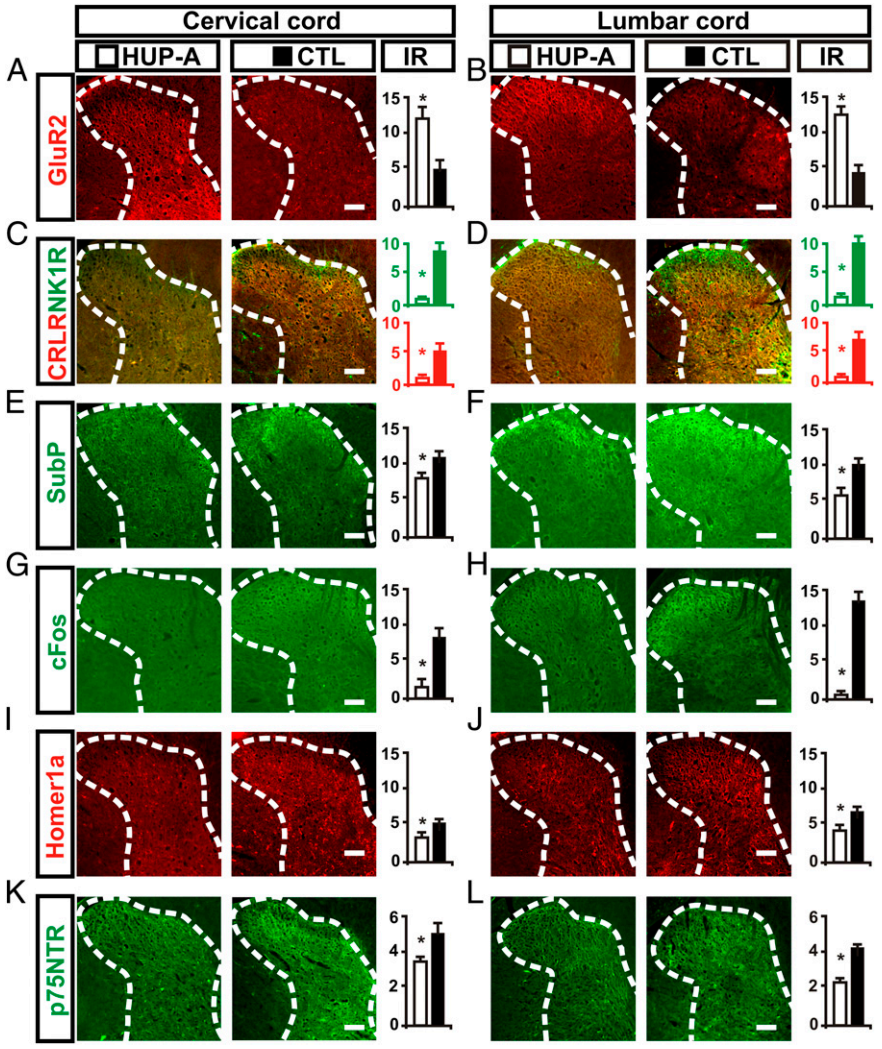

Fig. 6. HUP-A administration significantly inhibited nociceptive signaling in the cervical and lumbar spinal cord, albeit to a lesser degree in the cervical segment relatively distant from the lesion site. (*A* and *B*) Average expression of the GluR2 subunit of the AMPA receptor was higher in HUP-A–treated lumbar and cervical spinal cords. (*C* and *D*) CRLR and NK1R receptor expression in the DH was significantly lower in HUP-treated rats. (*E* and *F*) Substance P expression in the DH was decreased in HUP-treated rats. (*G* and *H*) cFos expression indicates decreased neuronal activity in the dorsal horn of the cervical and lumbar spinal cords of HUP-A-treated rats. (*I* and *J*) Average immunoreactive level of Homer1a, an endogenous protein with an important role in synaptic plasticity through an activity-dependent remodeling of the postsynaptic density in DH sensory neurons of the spinal cord, was significantly lower in HUP-A–treated rats. (*K* and *L*) Average immunoreactive level of neurotrophin receptor p75NTR also was significantly lower in HUP-A–treated rats, suggesting decreased neurite sprouting that also may contribute to the better-maintained sensory threshold (34). *$P < 0.05$, Student *t* test. (Scale bars: 100 μm.)

tolerated in general, because of their severe side effects on the gastrointestinal system (23), the bolus i.p. or continuous i.t. HUP-A dosing regimens tested in the present study did not cause discernible adverse gastrointestinal effects. The presumed reduced activity of DH pain-transmission neurons is supported further by our observation of better-maintained immunoreactivity levels of GluR2 in DH laminae I–III (Fig. 6 *A* and *B*). The death of neurons after SCI is referable in part to excitotoxicity and resultant GluR2 loss, which increases the permeability of these neurons to Ca^{2+} (32).

These combined actions together with reversible NMDA antagonism gave HUP-A high anti-hypersensitivity efficacy in our SCI model. Such a multimodal modulatory role of HUP-A may provide a strategy for pain management with minimal potential for the development of drug tolerance and dependence. This reasoning is supported by recent studies in which coadministration of the cholinesterase inhibitor donezepil and an initially ineffective dose of the adrenergic analgesic dexmedetomidine elicited anti-hypersensitivity effects in a rat model of peripheral neuropathic pain (41), and cell transplantation provided GABAergic interneurons that inhibited dysesthetic central pain after excitotoxic SCI (39).

In addition to demonstrating modulatory effects on neurotransmission, we showed that chronic cholinergic stimulation by HUP-A resulted in plasticity of spinal cord nociceptive circuitry that may facilitate lasting analgesia. Homer1a is the short form of the scaffolding proteins in the Homer1 family that can disrupt the mGluR signaling complex and negatively regulate nociceptive plasticity through an activity-dependent remodeling of the postsynaptic density in spinal cord sensory neurons (33). Thus, unlike approaches for pain management that aim to increase Homer1a expression in nociceptive relay neurons (33, 42), we found that HUP-A reduces the release of primary sensory neurotransmitters and inhibits secondary sensory neurons, preventing up-regulation of Homer1a in the DH (Fig. 6 *I* and *J*). This effect perhaps could be triggered additionally by HUP-A's an-

tagonist action on the NMDA receptor, similar to the inhibitory action of the NMDA receptor antagonist MK-801 on Homer1a observed in rat peripheral neuropathic pain and thermal hyperalgesia (42). HUP-A–mediated reduction of DH neuronal activity also is evidenced by the reduced expression of IEG cFos (Fig. 6 *G* and *H*) and p75 neurotrophin receptor (i.e., reduced neurite sprouting) in DH laminae I–III (Fig. 6 *K* and *L*), both of which are largely dependent on neuronal activity (43). Likewise, HUP-A–mediated postsynaptic inhibition (44) may be responsible for the observed down-regulation of the CRLR and the NK1R in DH sensory neurons (Fig. 6 *C* and *D*). These two types of receptors mediate pain-signal transmission for calcitonin gene-related peptide and substance P, respectively, suggesting that HUP-A triggers activity-dependent plasticity events in the dorsal spinal cord (44).

We hypothesized that HUP-A treatment also would impede post-SCI development of hypersensitivity through an anti-inflammatory effect, because acetylcholine inhibits the activation of macrophages/microglia (45–47) and astrocytes (48) via the α7 nAChR. Onset and chronic maintenance of neuropathic pain behavior depends, at least in part, on persistent microglial activation and secretion of inflammatory mediators (25, 49, 50). Indeed, we observed decreased ICC staining for activated microglia and $CD86^{+}$ M1 macrophages, decreased astrogliosis, and decreased expression of iNOS [a key enzyme involved in the generation of reactive oxidative species during inflammation (28)] in rats treated with HUP-A (Fig. 5 *C* and *D*). Additionally, our data suggest that the different effects of HUP-A on immunoreactivity of CD68, iNOS, and CD86 in the cervical compared with the lumbar segments may reflect varying degrees of involvement of the several cell types and reactive molecules in triggering above-injury-level or below-injury-level hyperalgesia (Fig. 5) (29). These findings, in addition to underlying the continued analgesic effect observed during the third week of HUP-A i.t. treatment (i.e., 1 wk after drug pump exhaustion), provide a perspective on the treatment of reactive astroglial neuropathic pain, because previous studies on cholinergic analgesia focused on acute effects on neurotransmission by nociceptive neurons and did not address the pathophysiological modulation of other spinal cord cell types that contribute to neuropathic hypersensitivity (15, 16, 20, 41). In parallel with the decrease in neuroinflammation, we observed mitigation of chronic demyelination in the HUP-A–treated spinal cord (Fig. 5 *G*–*J*). Axonal demyelination occurs simultaneously with disruption of gene expression for several types of sodium channels and contributes to chronic pain (51). Conversely, our HUP-A treatment regimen did not reduce significantly the loss of tissue volume (Fig. 4*B*) and motoneurons (Fig. 4*C*), nor did it improve axonal regeneration or motor function indices such as open-field locomotion (Fig. 5 *K* and *L*) or coordinated body posture control (Fig. 3 *E*–*H*). Because NMDA-mediated excitotoxicity plays primary roles in acute SCI, future studies should test if HUP-A administration in the early phase of SCI might reduce secondary tissue injury and motor dysfunction (24).

In summary, our findings suggest that HUP-A represents a multimodal therapeutic for managing clinical neuropathic pain after SCI and perhaps other neurological disorders including traumatic brain injury. Comprehensive approaches simultaneously modulating inhibitory tone in the dorsal spinal cord, affecting multiple central neurotransmission pathways, triggering neuroplasticity, and impeding inflammation may provide a powerful general strategy for developing drugs to treat chronic pain (Fig. 7).

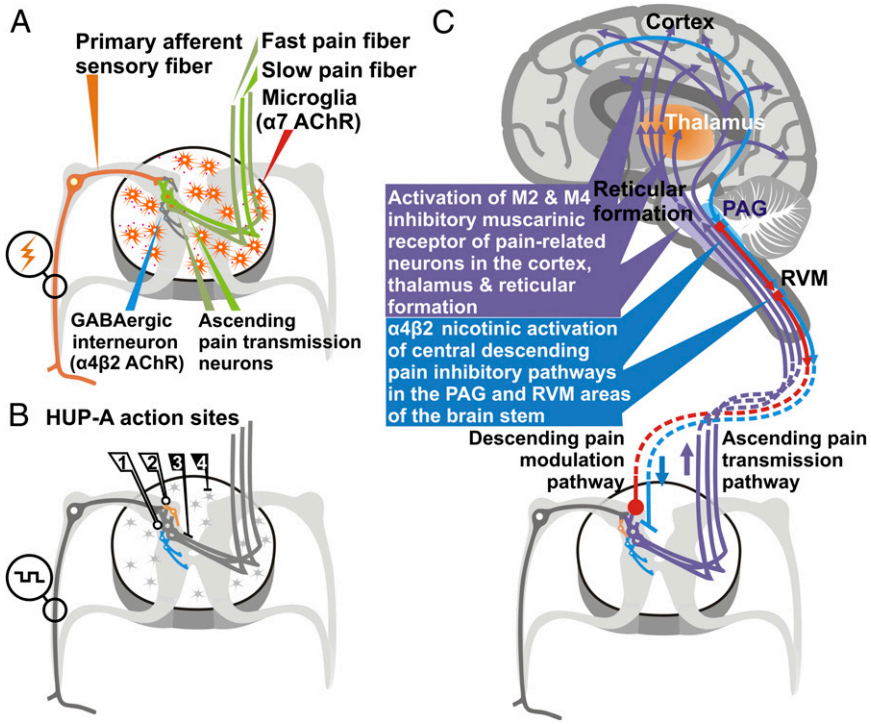

Fig. 7. Schematic presentation of putative multimodal action sites of HUP-A along the sensory and pain control pathways. (*A*) Primary pathophysiological components involved in triggering neuropathic pain and the inhibitory mechanisms that can be targeted at the spinal cord level by HUP-A to impede hypersensitivity. (*B*) HUP-A treatment modulates pain pathway by (1) activating inhibitory interneurons to mitigate firing of the secondary sensory neurons; (2) invoking presynaptic inhibition to reduce neurotransmitter release from primary sensory axons; (3) blocking NMDA receptors in the spinal cord sensory neurons; and (4) ameliorating inflammation by impeding microglial activation. (Note: potential neuroplastic events are not depicted in the diagrams.) (*C*) Sensory modulation sites along the supraspinal ascending and descending pathways that, in principle, can be targeted by HUP-A to control neuropathic pain. PAG, periaqueductal gray; RVM, rostral ventromedial medulla.

Materials and Methods

Surgical Model of Moderate Static Compression SCI. All procedures were evaluated and approved by the Institutional Animal Care and Use Committee of Harvard Medical School. Young adult female Sprague–Dawley rats (200–235 g body weight, n = 20; Taconic) were anesthetized with ketamine (75 mg/kg i.p.) and xylazine (10 mg/kg i.p.) before operation. Under a surgical stereomicroscope, dorsal laminectomy at thoracic vertebra 10 (T10) was performed to expose the spinal cord. After hemostasis was induced with Gelfoam (Pfizer), the rat body was suspended with a Teng Laboratory spine stabilization frame (fabricated at the Scientific Instrument Shop, Harvard University School of Engineering and Applied Sciences, Cambridge, MA), with 1-cm clearance between the ventral side of the rat and the frame base platform. A 35-g stainless steel impounder was lowered gently upon the dura surface via a micromanipulator, and the entire weight was allowed to compress the cord for 5 min (Fig. 1*E*). The lesion zone then was closed with sutures and stainless wound clips (Fine Science Tools Inc.), and the rat was allowed to recover in a clean, heated cage. Lactated Ringer's solution (10 mL/d, s.c.) was given daily for 5 d postoperation, and the urinary bladder was evacuated manually without urinary catheterization twice daily until reflex bladder function became reestablished (24).

HUP-A Preparation and Treatment. HUP-A [5R(5a,9b,11E)]-5-amino11ethlidene-5,6,9,10-tetrahydro-7-methyl-5,9-methanocycloocta[b]pyridin-2(1H)-one (molecular weight: 242.32; HPLC/UV purity: 98%; specific rotation: −152.8°; appearance: white powder] (Fig. 1*A*) was purchased from ChromaDex. Three weeks after SCI, HUP-A was administered as follows: (*i*) for the i.p. study (bolus dose treatment, n = 4): After sterile saline (2 mL per rat, i.p.) administration together with subsequent behavioral evaluation to obtain vehicle-control outcome measures, HUP-A, dissolved in 10% beta cyclodextrin in sterile saline (Sigma-Aldrich) at a concentration of 10 μg/μL before saline dilution to the final dose of 500, 167, or 50 μg/kg in a 2-mL bolus volume per rat for three treated groups, respectively (20), was administered. The injection was done with syringe needle passing 5 mm upward in the subdermal layer before penetrating through the muscle and peritoneal membrane layer to prevent postinjection leak and a brief withdrawal of the plunger to ensure no blood vessel piercing. After each dosing of saline followed with HUP-A (i.e., 500, 167, and 50 μg/kg with intervals of 24 h and 48 h, respectively), tests were performed using standard behavior batteries (see below). (*ii*) Implantation of the i.t. osmotic pump for chronic 2-wk treatment: HUP-A dissolved in 10% beta cyclodextrin in sterile saline (Sigma-Aldrich) was loaded in Alzet osmotic pumps (Durect Corporation) at a final dose per pump of 90 μg/168 μL to provide a 14-d i.t. continuous supply (pumping rate: 0.5 μL/h; total dose: 12 μL/d × 14 d = 168 μL). After reanesthetization and a small incision to expose the L5–L6 space, a dura puncture was made by an 18-G needle. A PE20 sterile catheter was inserted through the puncture with the beveled tip facing rostrally and was secured with a suture after a brief sign of tail flick was elicited by a light touch of nerve roots in the cauda equina to confirm proper i.t. penetration. The catheter was prefilled with 12 μL of sterile saline before the insertion and was connected to an osmotic pump filled with either HUP-A (treatment group; n = 7) or sterile saline containing 10% beta cyclodextrin (control group, n = 7). The tubing also was sutured to the fascia and musculature near the connection site with the s.c. embedded pump. The skin incision was closed with stainless steel wound clips, and standard postprocedure care was given (52). It took ∼24 h at a pumping rate of 0.5 μL/h, for HUP-A or saline to start entering the i.t. space. We first validated the effectiveness of the i.t. delivery by microinjection of 10 μL of 0.2% trypan blue via PE20 tubing in a pilot experiment (n = 2). (*iii*) I.t. redosing and atropine administration: The first round of HUP-A i.t. delivery was followed by a 2-wk "wash-out" period to permit the HUP-A effect to subside. We then started a second cycle of HUP-A treatment by replacing the HUP-A pump. The same sets of behavioral assays were performed, and 20 d later we administered a bolus dose of atropine (15 μg/10 μL, i.t. at L5–L6) to determine the effect of muscarinic antagonism on analgesic impact of HUP-A.

Behavioral Monitoring. A battery of behavioral tests was performed by observers blinded to the treatments on the day before the surgery, 1 d after SCI, and weekly thereafter to assess functional deficits and nociceptive changes. These tests evaluated open-field locomotion based on the BBB scale, the ability to maintain coordinated posture control on an inclined plane, the contact-righting reflex, the hindpaw-placing reflex, and the withdrawal reflex in response to pinch and pressure. In addition, after 30 min acclimation, the rats were subjected to a paw hyperalgesia test (modified von Frey filament test) to compare the withdrawal threshold before and after SCI or treatments, followed by hourly testing for up to 8 h after i.p. HUP-A injection and for 1 d, 2 d, and weekly thereafter up to 4 wk posttreatment for the i.t. HUP-A delivery study. Using the data obtained, we determined that with the α value (probability of rejecting H_0 when H_0 is true) being set at 5%, an average sample value of 0.41 g (post-SCI baseline sensory threshold), mean test value (posttreatment) of 3.1 g, and group size of four rats, the statistical power (i.e., 1-β) equals ∼100%, indicating that the β value (i.e., the probability of not rejecting H_0 when H_0 is false) = ∼0. The BBB and paw hyperalgesia test data were analyzed by repeated-measures ANOVA and by Bonferroni post hoc tests for multiple group comparisons with Analyze-it Statistics (Analyze-it Software Ltd. on Excel (Microsoft) (24, 52).

Histopathological Analysis. Rats were killed with an overdose i.p. injection of anesthetics followed by intracardiac perfusion with 4% (wt/vol) paraformaldehyde (PFA) in 0.1 M phosphate buffer at pH 7.4. Brain and spinal cord were dissected carefully, postfixed in 4% (wt/vol) PFA overnight at room temperature, dehydrated in 30% (wt/vol) sucrose at 4 °C for 24 h, and frozen in isopentane (Sigma-Aldrich) at −45 °C. The tissue then was encased in OCT compound (Sakura Finetek) and cryosectioned transversely at 20 μm. Sections representative of each millimeter of the spinal cord at and around the injury epicenter were chosen for solvent blue (a myelin stain, similar to luxol fast blue)/hematoxylin (S/H; both from Sigma) staining for analysis of lesion volume and counting of motor neurons. Lesion volume was measured based on the S/H staining from the area of the visualized lesion region in each representative section per millimeter of tissue and was calculated based on total lesion length. The motor neuron count was carried out as previously described

Table 1. Antibodies used in immunocytochemical assays

Antibody against	Marker for	Species	Dilution	Source	Location
GFAP	Intermediate filament of astrocytes	Rabbit	1:2,000	Dakocytomation	Carpentaria, CA
CD68	Microglia activation	Mouse	1:250	EMD Millipore	Carlsbad, CA
iNOS	Inducible NOS expression	Rabbit	1:500	Santa Cruz Biotechnology	Santa Cruz, CA
Arginase1	M2 Macrophage	Mouse	1:250	Santa Cruz Biotechnology	Santa Cruz, CA
CD86	M1 Macrophage	Rabbit	1:250	Abcam	Cambridge, MA
CNPase	Developing and adult myelin	Mouse	1:400	Sigma-Aldrich	St. Louis, MO
MBP	Mature myelin	Chicken	1:100	EMD Millipore	Carlsbad, CA
GluR2	Ca^{2+} impermeable subunit of AMPA-R	Mouse	1:250	EMD Millipore	Carlsbad, CA
Homer1a	Dominant negative linking protein of mGluR-signaling complex	Goat	1:250	Santa Cruz Biotechnology	Santa Cruz, CA
NK1R	Neurokinin-1 receptor	Goat	1:250	Santa Cruz Biotechnology	Santa Cruz, CA
CRLR	Calcitonin receptor-like receptor	Rabbit	1:250	Santa Cruz Biotechnology	Santa Cruz, CA
Substance P	Neurotransmitter related to pain	Rabbit	1:250	EMD Millipore	Carlsbad, CA
Neurofila-ment M	Marker for neuronal axons	Rabbit	1:200	EMD Millipore	Carlsbad, CA
Neurofila-ment H	Marker for mature neuronal axons	Mouse	1:200	EMD Millipore	Carlsbad, CA
cFos	Activated by strong neural activity	Rabbit	1:250	Santa Cruz Biotech.	Santa Cruz, CA
p75NTR	Low-affinity NGF receptor	Mouse	1:2	Gift from Mary B. Bunge	University of Miami, Miami, FL

(52). The average results (n = 7 for each study group) were compared with a paired t test performed by the software described above.

ICC Analysis of Signaling Markers Posttreatment. Representative spinal cord cross-sections were selected from the thoracic region rostral to the SCI epicenter and from cervical and lumbar regions for ICC probing of the post-SCI development of neuroinflammation and mechanistic markers of neuropathic pain pathways involved in post-SCI hyperalgesia. Sections were washed with PBS containing Triton X-100 (0.3%) and incubated in 5% (vol/vol) normal donkey serum. The primary antibodies used are listed in Table 1. Secondary antibodies were from Jackson ImmunoResearch Laboratories Inc. Slides were coverslipped using mounting medium containing DAPI (Vector LabsA) for imaging with an Axiovert200 microscope and digital Axiocam camera (Carl-Zeiss Microimaging) or with a Zeiss LSM1 confocal microscope equipped with Zeiss Zen 2011 software (Carl-Zeiss Microimaging). Semiquantification of positive ICC signals was performed with ImageJ (National Institutes of Health) and Photoshop (Adobe) software. A threshold signal-level range was determined by averaging the pixel brightness of the background and the strongly labeled structures, and the percentage of positively labeled pixels within the visual field was calculated to indicate the overall signal strength in the stained tissue. After confirmation of size compatibility for selected regions between samples, the average pixel numbers of ICC-positive labeling of a specific marker were compared in the treated and control groups (n = 7 per group) with a Student t test.

ACKNOWLEDGMENTS. This work was supported by grants from the Center for Integration of Medicine and Innovative Technology under US Army Medical Research Acquisition Activity Cooperative Agreement DAMD-17-02-2-0006 (to Y.D.T., S.C.S., and R.Z.) and by Grant B7076R from the Veterans Administration Rehabilitation Research and Development Service (to Y.D.T.).

1. Siddall PJ, McClelland JM, Rutkowski SB, Cousins MJ (2003) A longitudinal study of the prevalence and characteristics of pain in the first 5 years following spinal cord injury. *Pain* 103(3):249–257.
2. Oatway MA, Chen Y, Weaver LC (2004) The 5-HT3 receptor facilitates at-level mechanical allodynia following spinal cord injury. *Pain* 110(1-2):259–268.
3. Hama A, Sagen J (2009) Antinociceptive effects of the marine snail peptides conantokin-G and conotoxin MVIIA alone and in combination in rat models of pain. *Neuropharmacology* 56(2):556–563.
4. Hulsebosch CE, et al. (2000) Rodent model of chronic central pain after spinal cord contusion injury and effects of gabapentin. *J Neurotrauma* 17(12):1205–1217.
5. Hains BC, Waxman SG (2007) Sodium channel expression and the molecular pathophysiology of pain after SCI. *Prog Brain Res* 161:195–203.
6. Hains BC, et al. (2003) Upregulation of sodium channel Nav1.3 and functional involvement in neuronal hyperexcitability associated with central neuropathic pain after spinal cord injury. *J Neurosci* 23(26):8881–8892.
7. Leem JW, Kim HK, Hulsebosch CE, Gwak YS (2010) Ionotropic glutamate receptors contribute to maintained neuronal hyperexcitability following spinal cord injury in rats. *Exp Neurol* 224(1):321–324.
8. Hains BC, Waxman SG (2006) Activated microglia contribute to the maintenance of chronic pain after spinal cord injury. *J Neurosci* 26(16):4308–4317.
9. Jones PG, Dunlop J (2007) Targeting the cholinergic system as a therapeutic strategy for the treatment of pain. *Neuropharmacology* 53(2):197–206.
10. Patocka J (1998) – A—an interesting anticholinesterase compound from the Chinese herbal medicine. *Acta Med (Hradec Kralove)* 41(4):155–157.
11. Rafii MS, et al.; Alzheimer's Disease Cooperative Study (2011) A phase II trial of huperzine A in mild to moderate Alzheimer disease. *Neurology* 76(16):1389–1394.
12. Raves ML, et al. (1997) Structure of acetylcholinesterase complexed with the nootropic alkaloid, (-)-huperzine A. *Nat Struct Biol* 4(1):57–63.
13. Gordon RK, et al. (2001) The NMDA receptor ion channel: A site for binding of Huperzine A. *J Appl Toxicol* 21(Suppl 1):S47–S51.
14. Young T, Wittenauer S, McIntosh JM, Vincler M (2008) Spinal alpha3beta2* nicotinic acetylcholine receptors tonically inhibit the transmission of nociceptive mechanical stimuli. *Brain Res* 1229:118–124.
15. Cai YQ, et al. (2009) Role of M2, M3, and M4 muscarinic receptor subtypes in the spinal cholinergic control of nociception revealed using siRNA in rats. *J Neurochem* 111(4):1000–1010.
16. Kang YJ, Eisenach JC (2003) Intrathecal clonidine reduces hypersensitivity after nerve injury by a mechanism involving spinal m4 muscarinic receptors. *Anesth Analg* 96(5):1403–1408.
17. Rashid MH, Ueda H (2002) Neuropathy-specific analgesic action of intrathecal nicotinic agonists and its spinal GABA-mediated mechanism. *Brain Res* 953(1-2):53–62.
18. Park HJ, et al. (2007) Neuroprotective effect of nicotine on dopaminergic neurons by anti-inflammatory action. *Eur J Neurosci* 26(1):79–89.
19. Shytle RD, et al. (2004) Cholinergic modulation of microglial activation by alpha 7 nicotinic receptors. *J Neurochem* 89(2):337–343.
20. Park P, Schachter S, Yaksh T (2010) Intrathecal huperzine A increases thermal escape latency and decreases flinching behavior in the formalin test in rats. *Neurosci Lett* 470(1):6–9.
21. Wang Y, Wei Y, Oguntayo S, Doctor BP, Nambiar MP (2012) A combination of [+] and [-]-Huperzine A improves protection against soman toxicity compared to [+]-Huperzine A in guinea pigs. *Chem Biol Interact*, 10.1016/j.cbi.2012.10.016.
22. Pibiri F, et al. (2008) The combination of huperzine A and imidazenil is an effective strategy to prevent diisopropyl fluorophosphate toxicity in mice. *Proc Natl Acad Sci USA* 105(37):14169–14174.
23. Clayton BA, Hayashida K, Childers SR, Xiao R, Eisenach JC (2007) Oral donepezil reduces hypersensitivity after nerve injury by a spinal muscarinic receptor mechanism. *Anesthesiology* 106(5):1019–1025.
24. Teng YD, Mocchetti I, Taveira-DaSilva AM, Gillis RA, Wrathall JR (1999) Basic fibroblast growth factor increases long-term survival of spinal motor neurons and improves respiratory function after experimental spinal cord injury. *J Neurosci* 19(16):7037–7047.
25. Alexander JK, Popovich PG (2009) Neuroinflammation in spinal cord injury: Therapeutic targets for neuroprotection and regeneration. *Prog Brain Res* 175:125–137.
26. Hulsebosch CE (2008) Gliopathy ensures persistent inflammation and chronic pain after spinal cord injury. *Exp Neurol* 214(1):6–9.
27. Detloff MR, et al. (2008) Remote activation of microglia and pro-inflammatory cytokines predict the onset and severity of below-level neuropathic pain after spinal cord injury in rats. *Exp Neurol* 212(2):337–347.
28. Kigerl KA, et al. (2009) Identification of two distinct macrophage subsets with divergent effects causing either neurotoxicity or regeneration in the injured mouse spinal cord. *J Neurosci* 29(43):13435–13444.
29. Knerlich-Lukoschus F, von der Ropp-Brenner B, Lucius R, Mehdorn HM, Held-Feindt J (2011) Spatiotemporal CCR1, CCL3(MIP-1α), CXCR4, CXCL12(SDF-1α) expression patterns in a rat spinal cord injury model of posttraumatic neuropathic pain. *J Neurosurg Spine* 14(5):583–597.
30. Yaksh TL, et al. (2008) Toxicology profile of N-methyl-D-aspartate antagonists delivered by intrathecal infusion in the canine model. *Anesthesiology* 108(5):938–949.
31. Kopach O, et al. (2011) Inflammation alters trafficking of extrasynaptic AMPA receptors in tonically firing lamina II neurons of the rat spinal dorsal horn. *Pain* 152(4):912–923.
32. Grossman SD, Rosenberg LJ, Wrathall JR (2001) Relationship of altered glutamate receptor subunit mRNA expression to acute cell loss after spinal cord contusion. *Exp Neurol* 168(2):283–289.
33. Miletic G, Driver AM, Miyabe-Nishiwaki T, Miletic V (2009) Early changes in Homer1 proteins in the spinal dorsal horn are associated with loose ligation of the rat sciatic nerve. *Anesth Analg* 109(6):2000–2007.
34. Deumens R, Joosten EA, Waxman SG, Hains BC (2008) Locomotor dysfunction and pain: The scylla and charybdis of fiber sprouting after spinal cord injury. *Mol Neurobiol* 37(1):52–63.
35. Hama A, Sagen J (2012) Combination drug therapy for pain following chronic spinal cord injury. *Pain Res Treat*, 10.1155/2012/840486.
36. Jarvis MF, Boyce-Rustay JM (2009) Neuropathic pain: Models and mechanisms. *Curr Pharm Des* 15(15):1711–1716.
37. Dominguez CA, et al. (2012) Genetic and sex influence on neuropathic pain-like behaviour after spinal cord injury in the rat. *Eur J Pain* 16(10):1368–1377.
38. Hartrick CT, Gatchel RJ, Conroy S (2012) Identification and management of pain medication abuse and misuse: Current state and future directions. *Expert Rev Neurother* 12(5):601–610.
39. Lee JW, Jergova S, Furmanski O, Gajavelli S, Sagen J (2012) Predifferentiated GABAergic neural precursor transplants for alleviation of dysesthetic central pain following excitotoxic spinal cord injury. *Front Physiol*, 10.3389/fphys.2012.00167.
40. Harte SE, Hoot MR, Borszcz GS (2004) Involvement of the intralaminar parafascicular nucleus in muscarinic-induced antinociception in rats. *Brain Res* 1019(1-2):152–161.
41. Kimura M, Saito S, Obata H (2012) Dexmedetomidine decreases hyperalgesia in neuropathic pain by increasing acetylcholine in the spinal cord. *Neurosci Lett* 529(1):70–74.
42. Tappe-Theodor A, Fu Y, Kuner R, Neugebauer V (2011) Homer1a signaling in the amygdala counteracts pain-related synaptic plasticity, mGluR1 function and pain behaviors. *Mol Pain* 7:38.
43. Ezkurdia N, et al. (2012) Blockage of the afferent sensitive pathway prevents sympathetic atrophy and hemodynamic alterations in rat portal hypertension. *Liver Int* 32(8):1295–1305.
44. Smith MD, Yang XH, Nha JY, Buccafusco JJ (1989) Antinociceptive effect of spinal cholinergic stimulation: Interaction with substance P. *Life Sci* 45(14):1255–1261.
45. Rosas-Ballina M, Tracey KJ (2009) The neurology of the immune system: Neural reflexes regulate immunity. *Neuron* 64(1):28–32.
46. Carnevale D, De Simone R, Minghetti L (2007) Microglia-neuron interaction in inflammatory and degenerative diseases: Role of cholinergic and noradrenergic systems. *CNS Neurol Disord Drug Targets* 6(6):388–397.
47. de Jonge WJ, Ulloa L (2007) The alpha7 nicotinic acetylcholine receptor as a pharmacological target for inflammation. *Br J Pharmacol* 151(7):915–929.
48. Liu Y, et al. (2012) α7 nicotinic acetylcholine receptor-mediated neuroprotection against dopaminergic neuron loss in an MPTP mouse model via inhibition of astrocyte activation. *J Neuroinflammation* 9:98, 10.1186/1742-2094-9-98.
49. Milligan ED, Watkins LR (2009) Pathological and protective roles of glia in chronic pain. *Nat Rev Neurosci* 10(1):23–36.
50. Inoue K, Tsuda M (2009) Microglia and neuropathic pain. *Glia* 57(14):1469–1479.
51. Waxman SG (2012) Sodium channels, the electrogenisome and the electrogenistat: Lessons and questions from the clinic. *J Physiol* 590(Pt 11):2601–2612.
52. Teng YD, Mocchetti I, Wrathall JR (1998) Basic and acidic fibroblast growth factors protect spinal motor neurones in vivo after experimental spinal cord injury. *Eur J Neurosci* 10(2):798–802.